Microwave emission from snow: modeling the effects of volume scattering, surface scattering and layering

Leung Tsang[1], Ding Liang[1], Xiaolan Xu[1], and Peng Xu[2]

1. Department of Electrical Engineering, University of Washington, Seattle, USA
2. Center for Space and Remote Sensing Research, National Central University, Republic of China

MiCroRad2008, Florence, Italy, March 14th, 2008

Outline

1. Volume Scattering with Layering
   1. *Quasicrystalline Approximation (QCA/DMRT) simulate all 4 brightness temperature channels: 18V, 18H, 37 V and 37 H*
   2. *Polarization and frequency dependence*
   3. *Comparison with CLPX GBMR ground measurements for all 4 channels*
2. Volume Scattering
   1. *Numerical Maxwell Model based on 3D Solutions (NMM3D) of Maxwell equations*
   2. *Comparison between NMM3D/DMRT and QCA/DMRT*
3. Rough Surface Scattering with Layering : Numerical solutions of Maxwell Equations:
   1. *There can be Large 3rd and 4th Stokes due to interactions of rough surface with layering*
   2. *Large 3^{rd} and 4^{th} parameters observed in WINDSAT Data over Greenland*

Dense Media: Collective Scattering Effects

a) Snow: dense media ice grains lie in close proximity within a wavelength

b) Induced dipoles/multipoles have near field coherent interactions

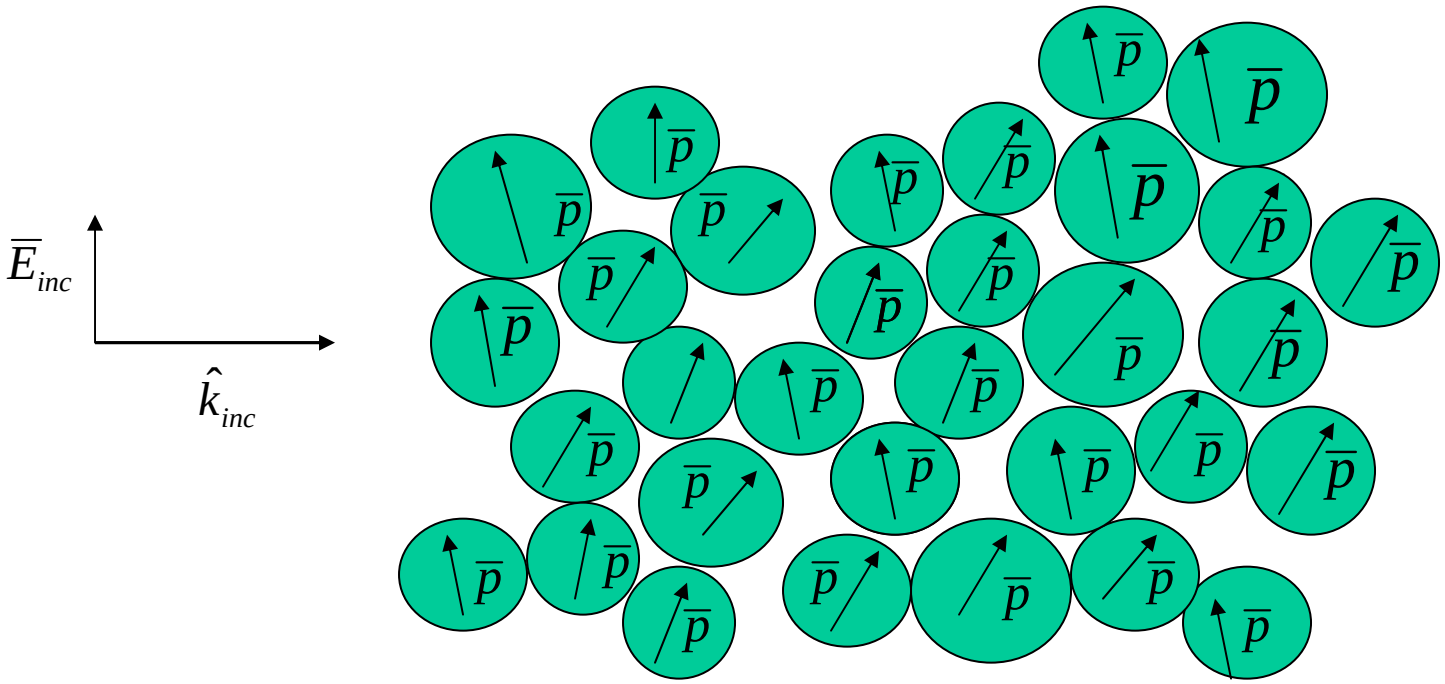

Quasicrystalline Approximation (QCA): Lorentz Lorenz law and Ewald Oseen Extinction Theorem

Lorentz-Lorentz law: $X^{(M)}$ and $X^{(N)}$: averaged multipole amplitudes; 2 Nmax number of equations

$$X_{\upsilon}^{(M)} = -2\pi n_0 \sum_{n,p} (2n+1)\lfloor Lp(k,K/b) + Mp(k,K/b)\rfloor \times \{T_n^{(M)} X_n^{(M)} a(1,n/-1,\upsilon/p) \times A(n,\upsilon,p) + T_n^{(N)} X_n^{(N)} a(1,n/-1,\upsilon/p,p-1) B(n,\upsilon,p)\}$$

$$X_{\upsilon}^{(N)} = -2\pi n_0 \sum_{n,p} (2n+1)\lfloor Lp(k,K/b) + Mp(k,K/b)\rfloor \times \{T_n^{(M)} X_n^{(M)} a(1,n/-1,\upsilon/p,p-1) \times B(n,\upsilon,p) + T_n^{(N)} X_n^{(N)} a(1,n/-1,\upsilon/p) A(n,\upsilon,p)\}$$

$$Mp(k,K/b) = \int_b^{\infty} dr r^2 [g(r)-1] h_p(kr)\, j_p(Kr)$$

$$Lp(k,K/b) = -\frac{b^2}{(K^2-k^2)} [k h_p'(kb)\, j_p(Kb) - K h_p(kb)\, j_b'(Kb)]$$

Ewald-Oseen theorem:

$$K - k = -\frac{\pi i n_0}{k^2} \sum_n (T_n^{(M)} X_n^{(M)} + T_n^{(N)} X_n^{(N)})(2n+1)$$

K, $X^{(M)}$ and $X^{(N)}$ are calculated by solving the L-L law and E-O theorem

Nmax=2 , Higher order multipole is used because of sticky aggregation effects

Comparison between QCA/DMRT and classical independent scattering

Extinction Rate frequency dependence Comparison:

QCA shows weaker frequency dependence than classical theory

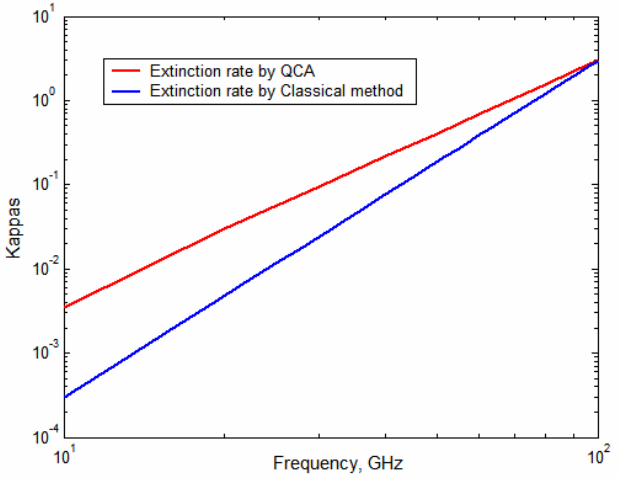

2a=1.2mm, fv=0.2

Extinction Rate fractional volume dependence comparison:

QCA simulation saturates with fractional volume

Classical theory simulation linearly increase fractional volume

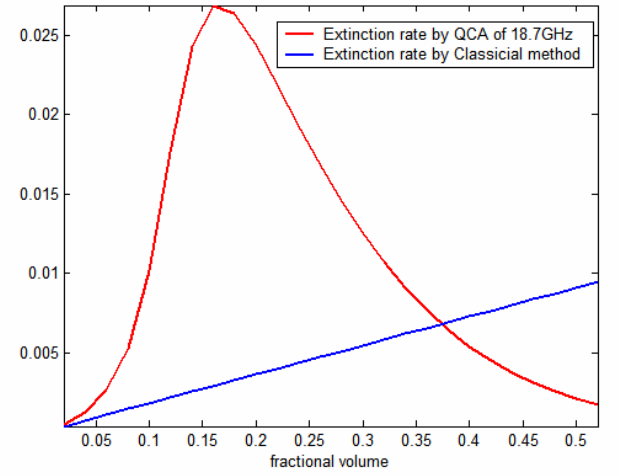

2a=1.2mm, freq=18.7GHz

Phased Matrix Comparison

For same grain size, QCA simulation shows more forward scattering than classical Mie theory

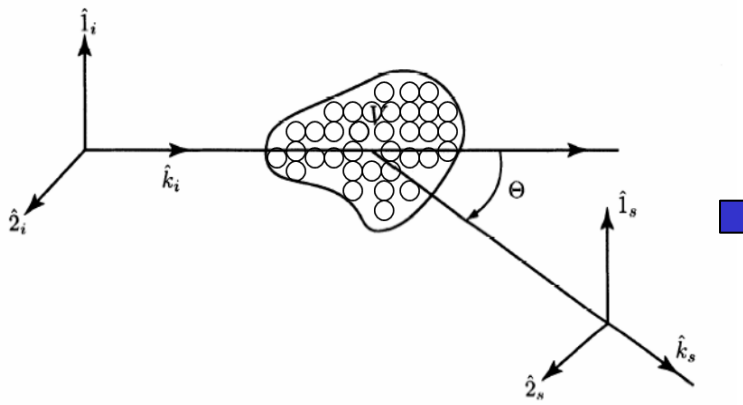

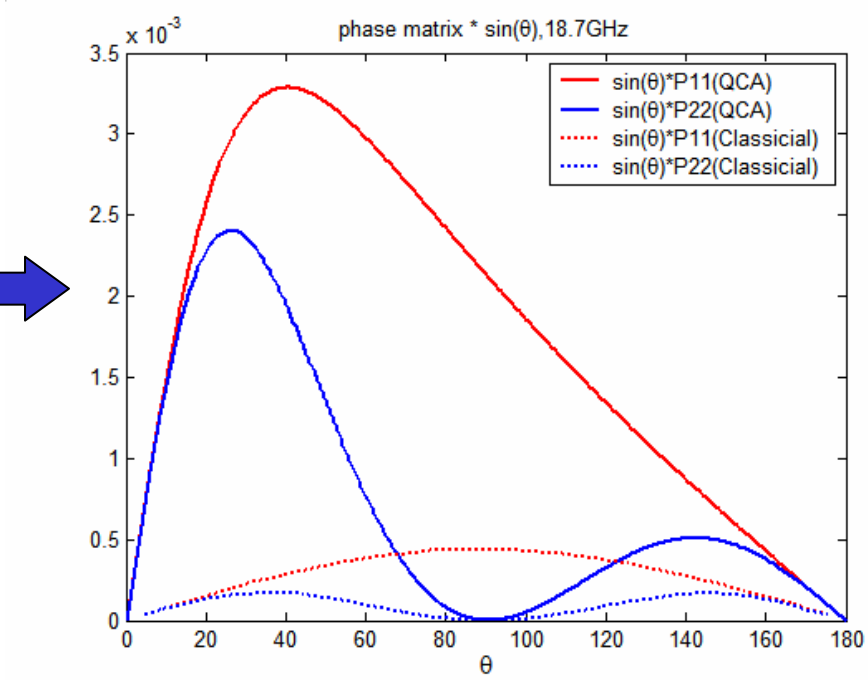

diameter=1.2mm, fractional volume=0.2, Freq=18.7GHz

Multi-layer Dense media radiative transfer

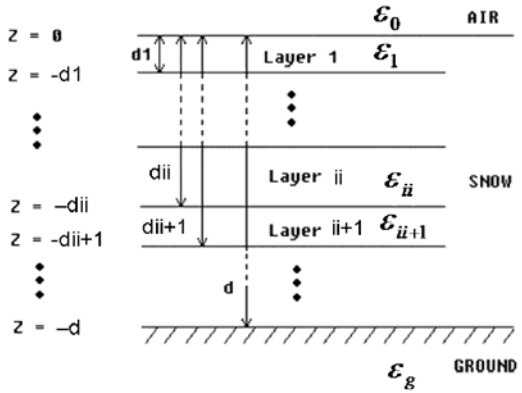

Passive Microwave Remote Sensing

N layers of snow with the ii th layer of snow from $z=-d_{ii-1}$ to $z=-d_{ii}$ $ii=1,2,...N$

Dense media radiative transfer equations in the ii th layer :

$$\cos\theta\frac{d\bar{I}_{ii}}{dz}=-\kappa_e^{ii}\cdot\bar{I}_{ii}+\kappa_a T^{ii}+\int_0^{\pi}d\theta'\sin\theta'\bar{\bar{P}}_0^{ii}(\theta,\theta')\cdot\bar{I}_{ii}(z,\theta')$$

The boundary conditions are

At $z=0$

$$\bar{I}_1(\pi-\theta,z=0)=\bar{\bar{R}}_{10}(\theta)\bar{I}_1(\theta,z=0)$$

At $z=-d_j$ $j=1,2,...N-1$

$$\bar{I}_j(\theta,z=-d_j)=\bar{\bar{R}}_{j,j+1}(\theta)\bar{I}_j(\pi-\theta,z=-d_j)+\bar{\bar{S}}_{j+1,j}(\theta)\bar{\bar{T}}_{j+1,j}(\theta)\bar{I}_{j+1}(\theta,z=-d_j)$$

$$\bar{I}_{j+1}(\pi-\theta,z=-d_j)=\bar{\bar{R}}_{j+1,j}(\theta)\bar{I}_{j+1}(\theta,z=-d_j)+\bar{\bar{S}}_{j,j+1}(\theta)\bar{\bar{T}}_{j,j+1}(\theta)\bar{I}_j(\pi-\theta,z=-d_j)$$

At $z=-d$

$$\bar{I}_n(\theta,z=-d)=\bar{\bar{R}}_{ng}(\theta)\bar{I}_n(\pi-\theta,z=-d)+\bar{\bar{T}}_{gn}(\theta)T_g$$

4 channels :18V, 18H, 37V and 37H
Polarization and frequency dependence

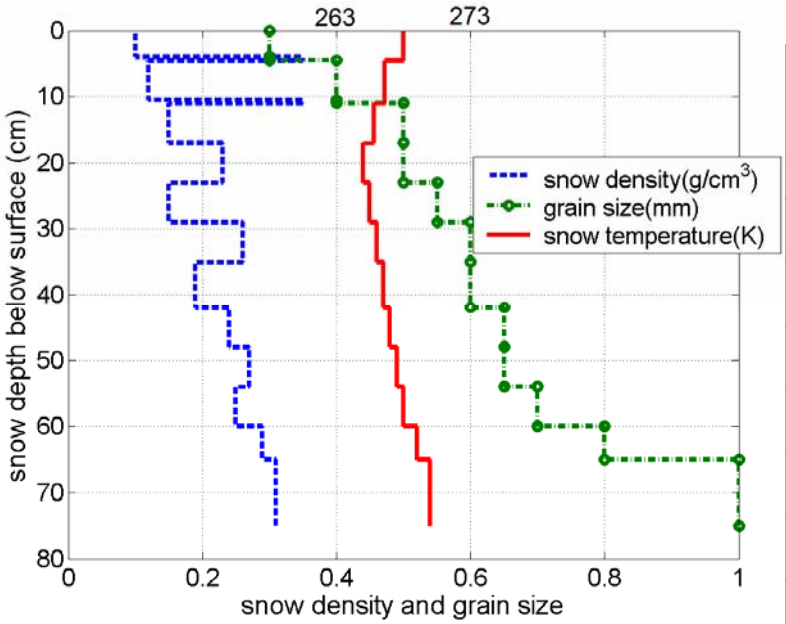

hypothetical, but realistic, snow packs

Tb simulation

channel	Single-layer smooth	Multi-layer smooth	Single-layer rough	Multi-layer rough
18.7v	241.3	241.2	240.5	240.9
18.7h	215.7	209	226.6	216.8
36.5v	207.4	208.9	207.6	209
36.5h	192.8	188.5	193.1	188.7
18.7v-18.7h	25.6	32.2	15.7	24.1
36.5v-36.5h	14.6	20.4	14.5	20.3
18.7v-36.5v	33.9	32.3	32.9	31.9
18.7h-36.5h	22.9	20.5	33.5	28.1

- snow densities fluctuate but generally increase as the snow depth increases
- Large density fluctuation near the surface is due to thin ice crusts near the surface
- snow grain sizes increase as the snow depth increases
- snow temperature decreases at first and then increases as the snow depth increases

Multi-layer model predicts larger polarization difference and smaller frequency dependence than a single-layer snow model

Brightness Temperature change with new snow accumulation on thin snow pack

dia=diameter (mm)
den=density(g/cm^3)

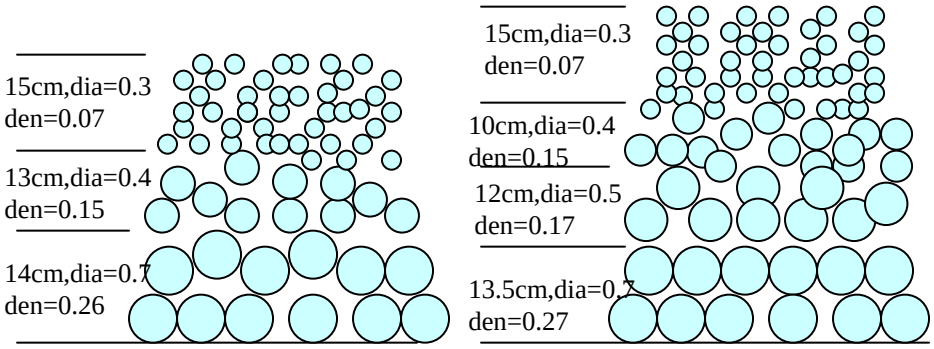

Profile 1 Profile 2

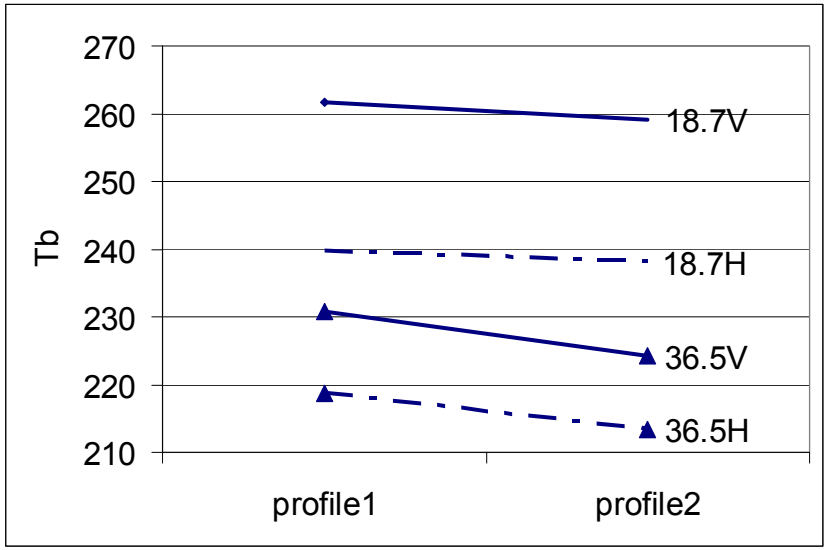

Tb for different profiles.

Hypothetical snow profiles of 2 days ; new snow in profile 1 turned to the 2nd layer in profile 2 after new snow accumulated in the 2nd day

Tb decreases as new snow accumulates on thin snow pack

CLPX Ground based Microwave Radiometer measurements

Location: CLPX Local-Scale Observation Site (LSOS), Colorado

Time:18-26 Feb. and 25 March 2003

Instrument: Ground Based Passive Microwave Radiometer (GBMR-7)

Frequency: 18.7GHz and 36.5GHz **Incident angles:** 54 degree

Data: Brightness temperature

LSOS snow pits location in 2003

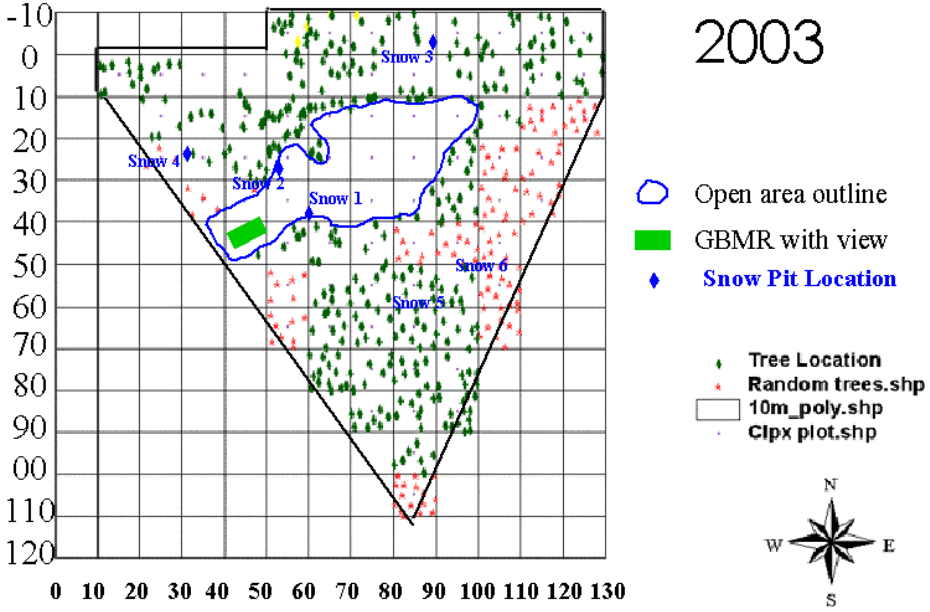

LSOS is a 100m×100m study site which has flat topography with a uniform pine forest, a discontinuous pine forest, and a small clearing

CLPX
snow profiles used as input to DMRT

Snow profiles of grain size, snow density and snow temperature of LSOS at Feb.21,2003

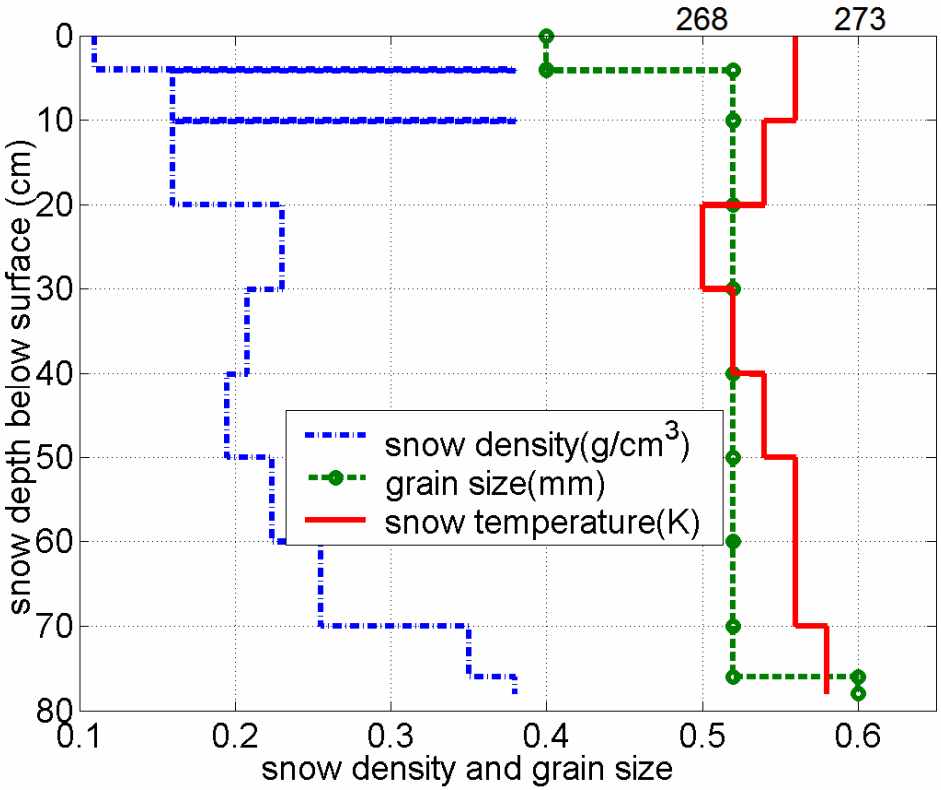

The snow profile based on snow pit measurements at snow pit #2 of CLPX.

The averaged snow parameters from Variable Infiltration Capacity (VIC) Macroscale Hydrologic Model simulations

Comparison with GBMR point Tb observations : all 4 channels

polarization differences and frequency differences

18.7GHz v-h; 36.5GHz v-h

TB comparisons

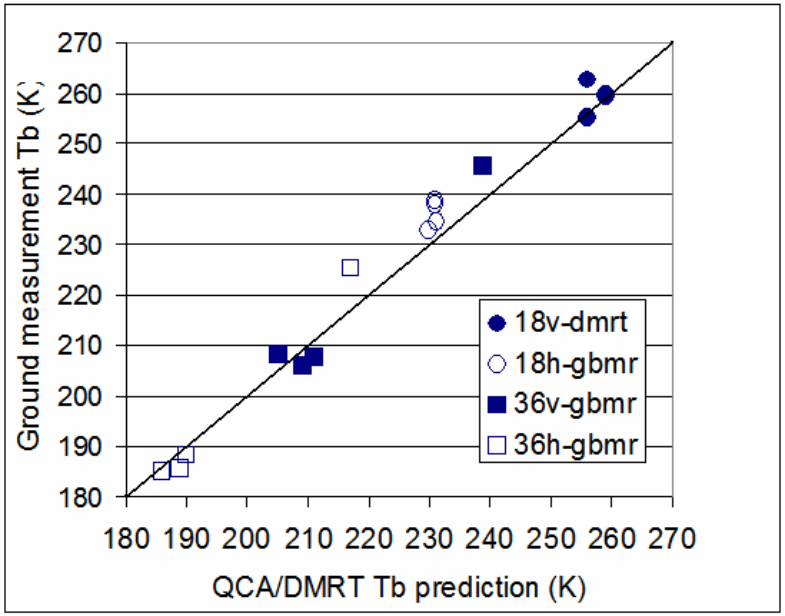

TB polarization difference and frequency difference comparisons

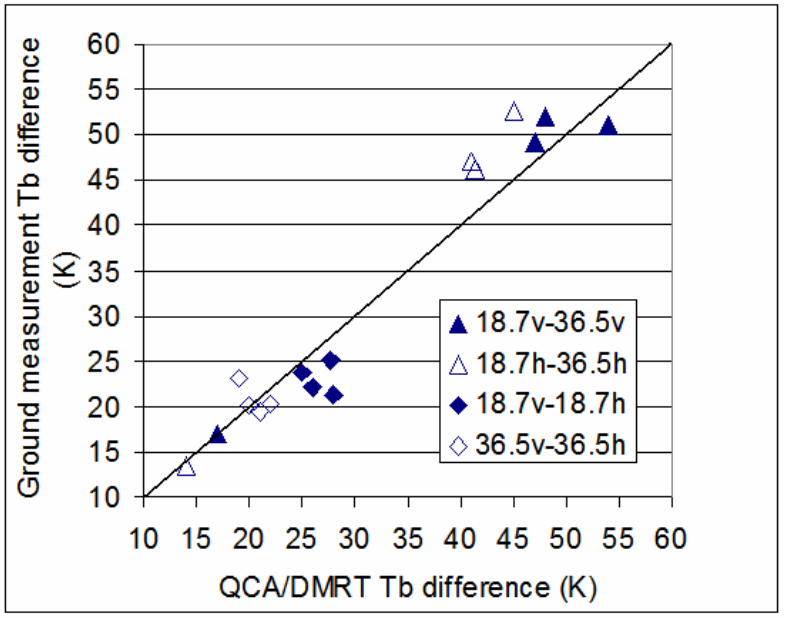

1)The model Tb prediction (left figure) show close agreement with the ground Tb observation.

2) Polarization difference (18.7v-18.7h and 36.5v-36.5h,right figure) from DMRT show close agreement with observations.

3) Frequency difference(18.7v-36.5v and 18.7h-36.5h, right figure) from DMRT show close agreement with observations.

4) Multilayer model better agreement with GBMR than single layer model

NMM3D
(Numerical Maxwell Model based on 3 D Solutions of Maxwell Equations)

- Computer generation of particles random shuffling and bonding, several thousands of particles
- Solve Maxwell equations numerically for the Generated Samples:
- Solutions of Maxwell equations fluctuates; results averaged over 20-25 solutions of sampl

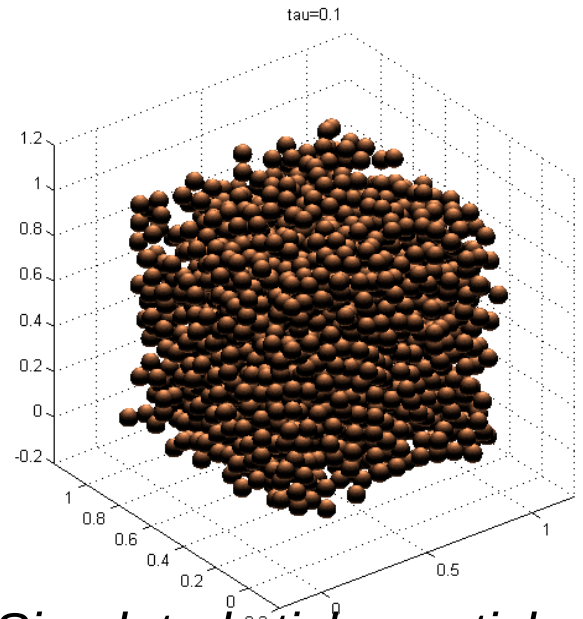

Simulated sticky particles
fv = 40%

Foldy-lax Multiple Scattering Equations

$$\bar{E}^{inc}(\bar{r}) = \sum_{m,n}\left[a_{mn}^{(M)} Rg\bar{M}_{mn}(kr,\theta,\phi) + a_{mn}^{(N)} Rg\bar{N}_{mn}(kr,\theta,\phi)\right]$$

$$\bar{E}_l^{ex}(\bar{r}) = \sum_{mn}\left[w_{mn}^{(M)(l)}\ Rg\bar{M}_{mn}(k\bar{rr_l}) + w_{mn}^{(N)(l)} Rg\bar{N}_{mn}(k\bar{rr_l})\right]$$

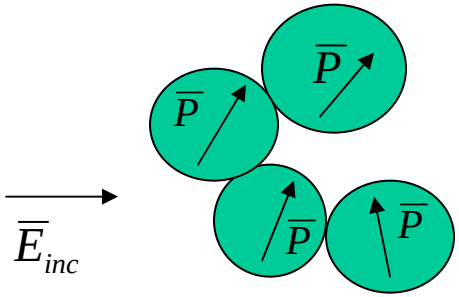

The field exciting a single particle is the sum of incident wave and scattered wave from all other scatterers except itself

$$\bar{E}_l^{ex} = \bar{E}^{inc} + \bar{\bar{G}}_0 \sum_{\substack{j=1 \\ j\neq l}}^{N} \bar{\bar{T}}_j \bar{E}^{ex}{}_j$$

Foldy-Lax equations:

$$\bar{w}^{(q)} = \sum_{\substack{p=1 \\ p\neq q}}^{N} \bar{\bar{\sigma}}(k\bar{r_q r_p})\bar{\bar{T}}^{(p)}\bar{w}^{(p)} + e^{i(\bar{k_i}\bullet\bar{r_q})}\bar{a}_{inc}$$

Comparison with Experiments :

Scattering Power Law dependence on Frequency

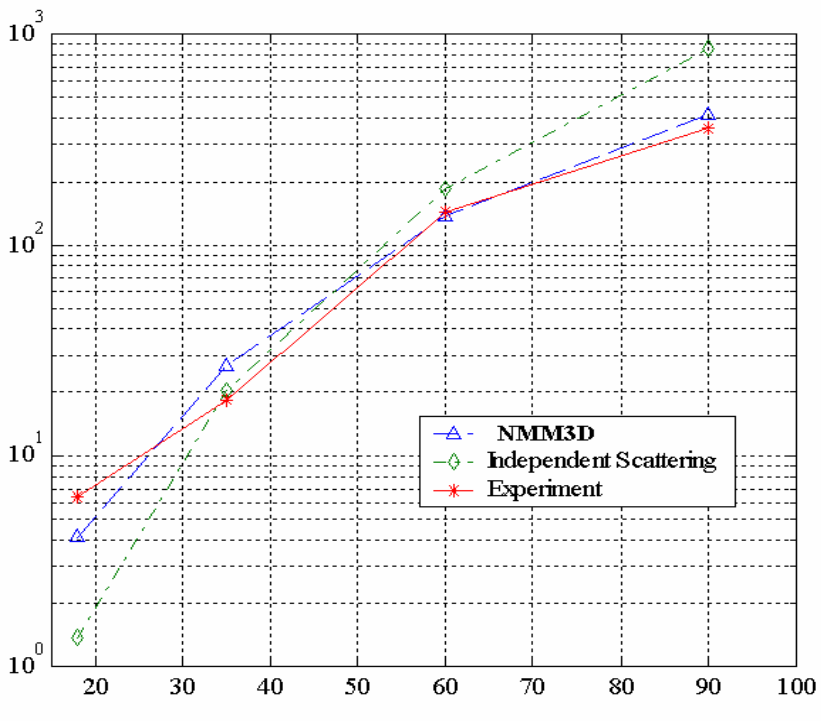

The frequency dependence index

$$n = \log\left[\frac{\kappa_s(at\ f_2)}{\kappa_s(at\ f_1)}\right] \Big/ \log\left(\frac{f_2}{f_1}\right)$$

Frequency (GHz)	18	35	60	90
NMM3D	-	2.79	3.04	2.75
Experiment	-	1.59	3.82	2.25
Independent Scattering	-	4.04	4.06	4.05

Phase Matrix, P11 and P22 : Comparison Between Classical ,QCA and NMM3D

- P11 and P22 (τ=0.1). Particles with diameter of 1.2mm ; 20% of volume fraction, 25 realizations,number of particles 2000
- Sticky particles (QCA,NMM3D) have larger scattering

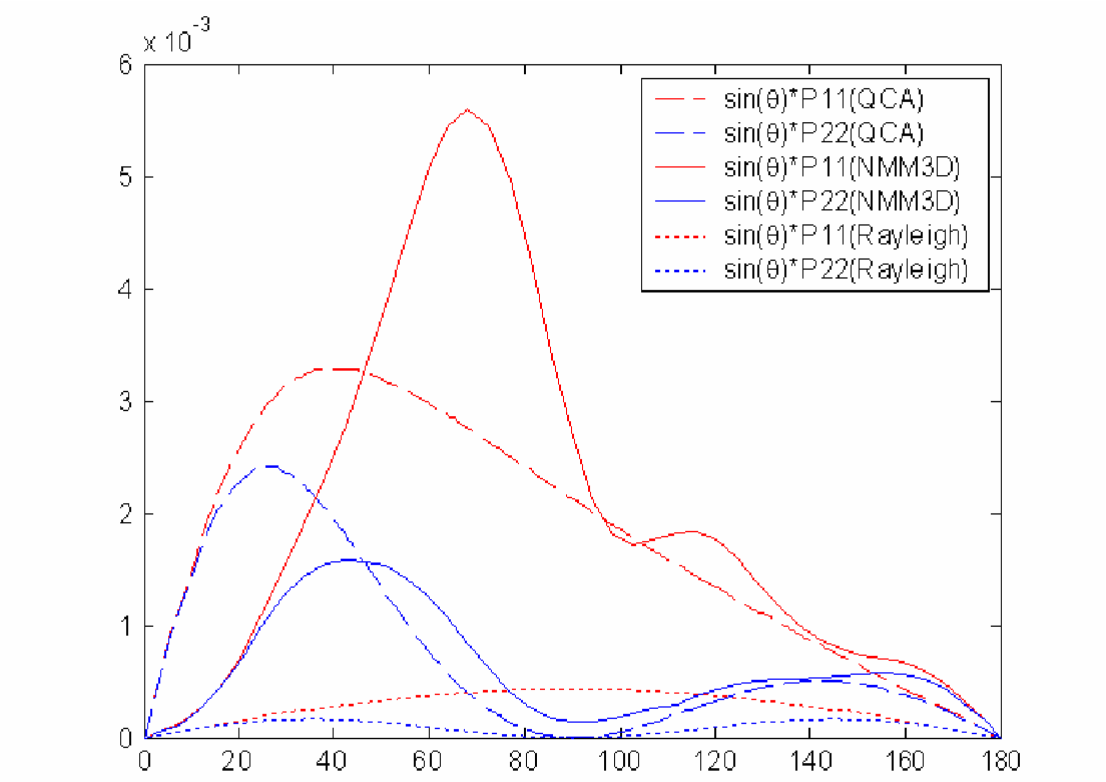

Extinction rate vs fractional volume

- Extinction rate : diameter = 1.2mm , stickiness τ=0.1 , frequency 18.7GHz and 37GHz.
- NMM3D in agreement with QCA up to 20%, but start to deviate at 30%

Frequency = 18.7GHz

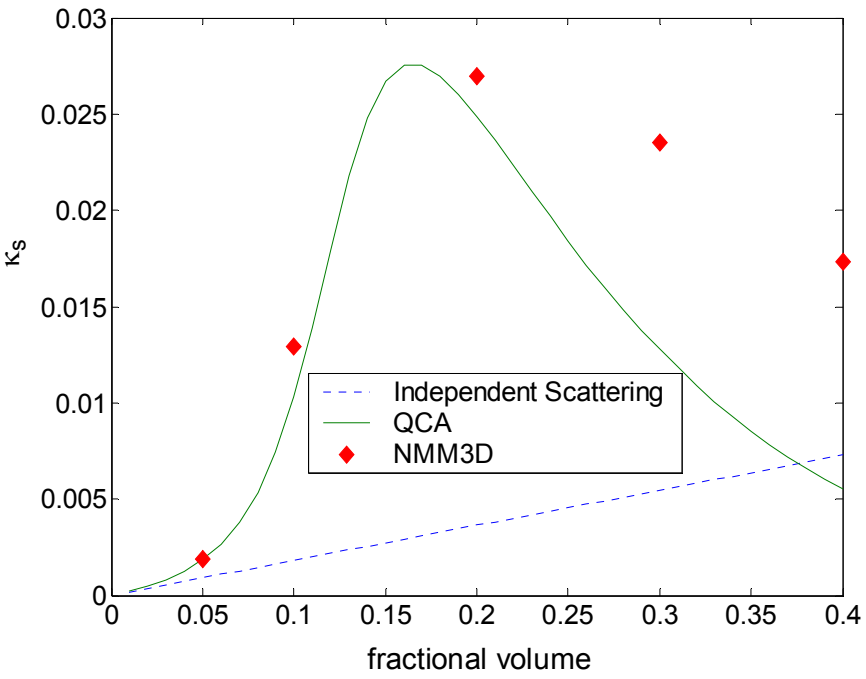

Frequency = 37GHz

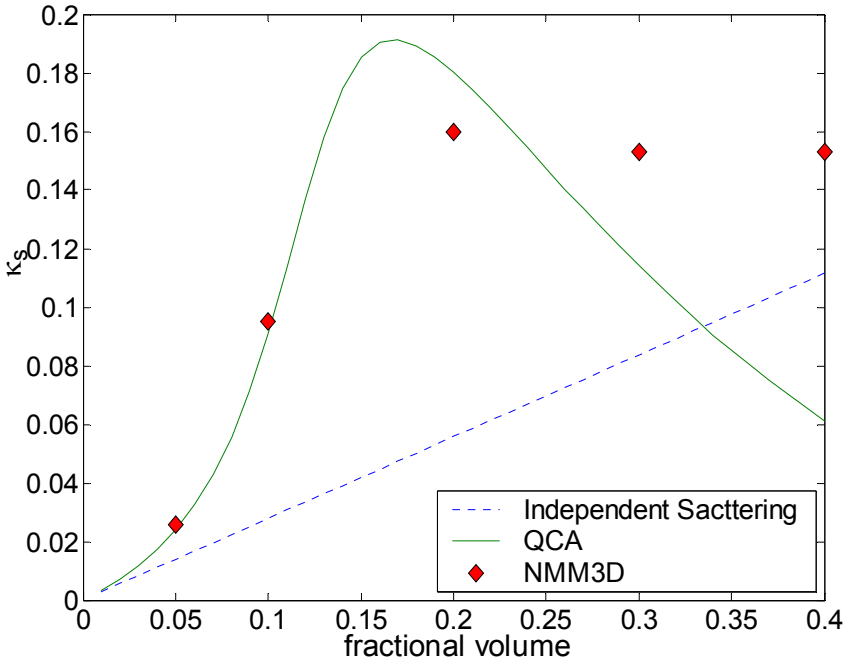

NMM3D-DMRT

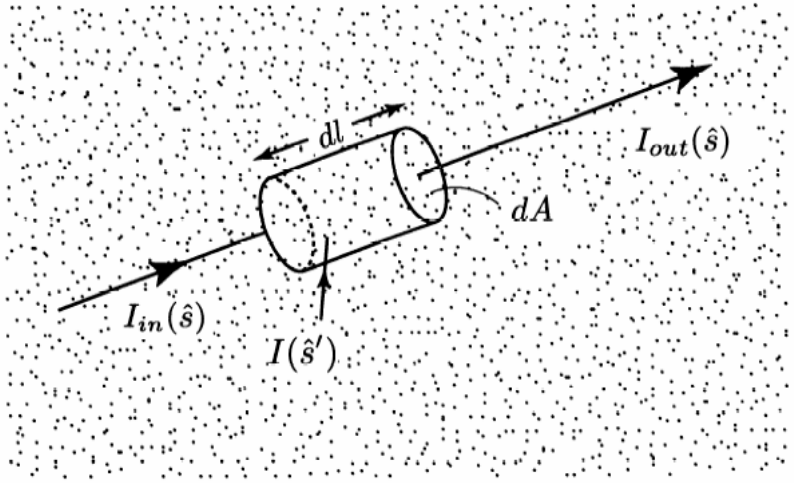

i) κ_e : extinction rate, $\kappa_e = \kappa_a + \kappa_s$

ii) κ_a : absorption rate, $\overline{\overline{P}}(\theta,\phi;\theta',\phi')$: NMM3D phase matrix (bistatic scattering coefficient per unit volume) from direction $\hat{s}'$ into direction $\hat{s}$

$$\cos\theta \frac{d\bar{I}(z,\theta,\phi)}{dz} = -\kappa_e \cdot \bar{I}(z,\theta,\phi) + \kappa_a T + \int_0^{2\pi}\int_0^{\pi} d\theta' d\phi' \sin\theta' \overline{\overline{P}}(\theta,\phi;\theta',\phi')\bar{I}(z,\theta',\phi')$$

Tb comparisons
QCA/DMRT and NMM3D/DMRT

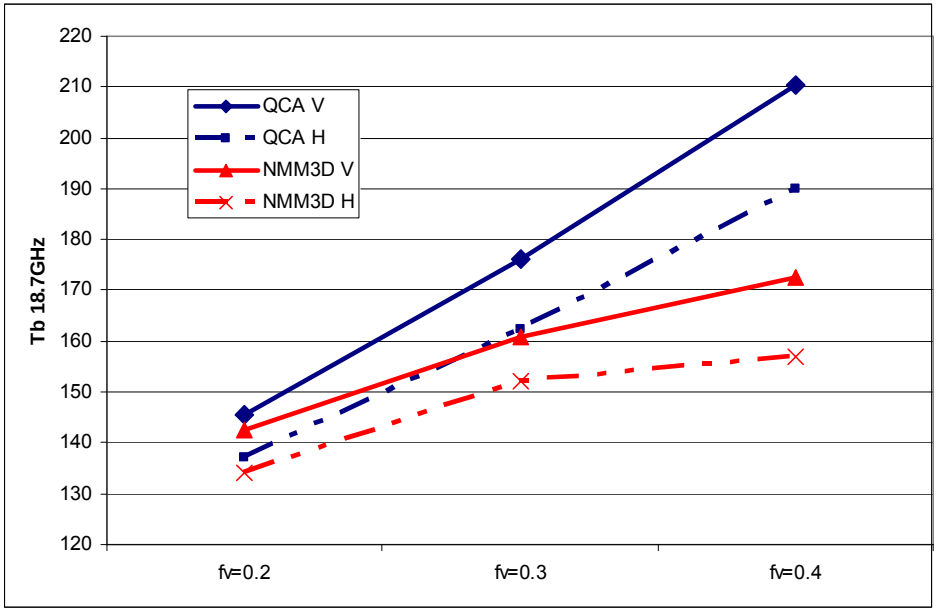

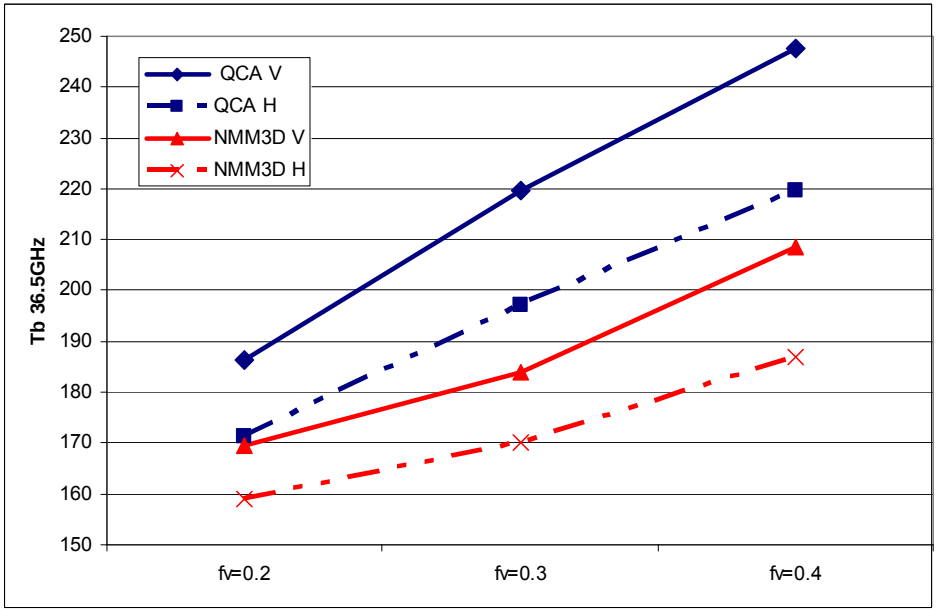

For fixed grain size, NMM3D shows weaker fractional volume dependence
Of Tb than QCA

Rough Surface over Layered Media

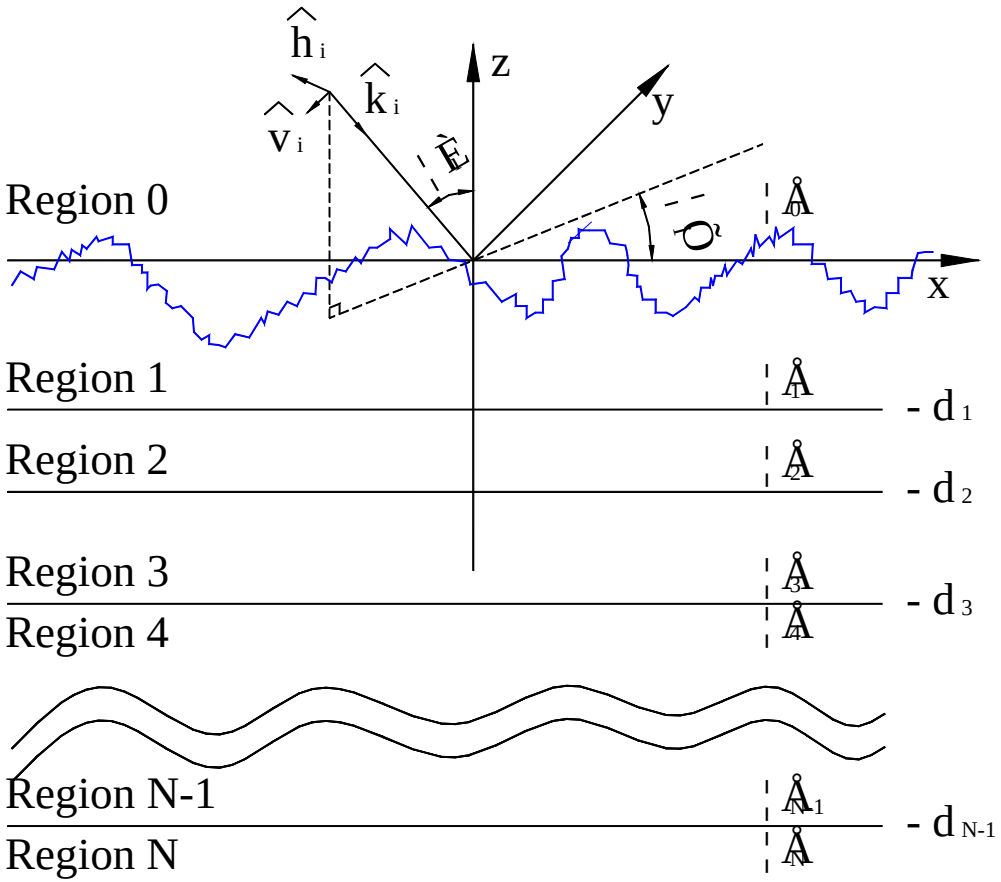

WindSat data over Greenland

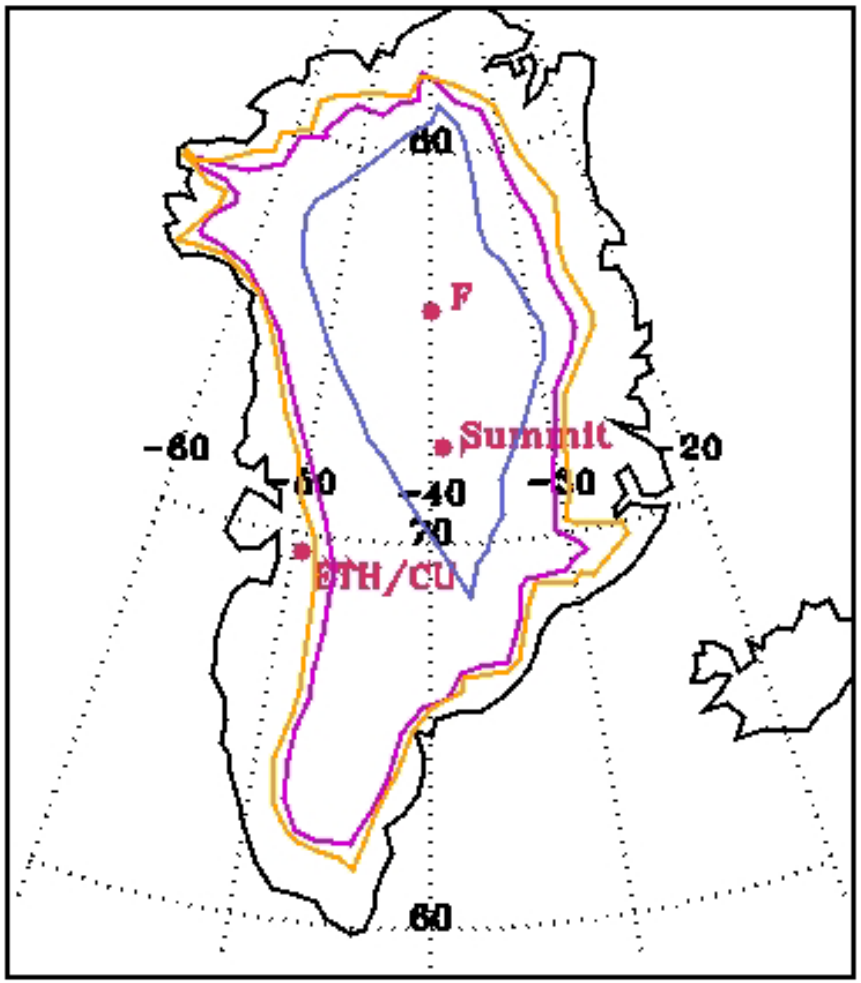

Greenland map showing study site locations for WindSat data

Third Stokes parameter

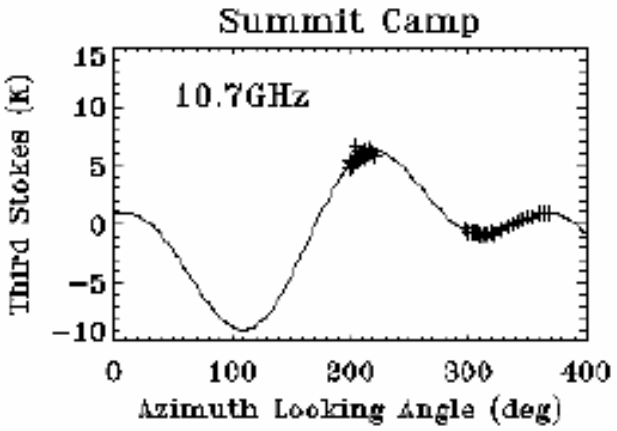

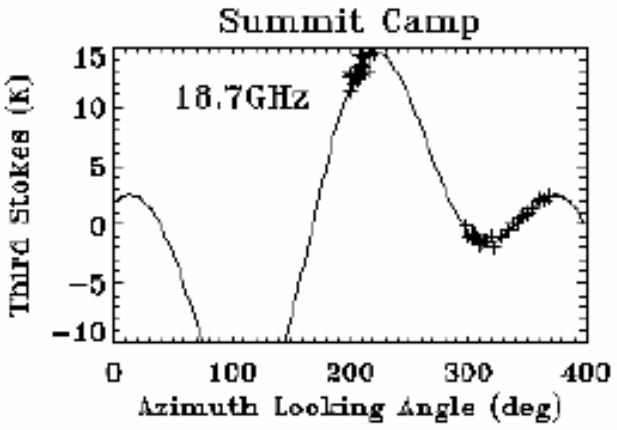

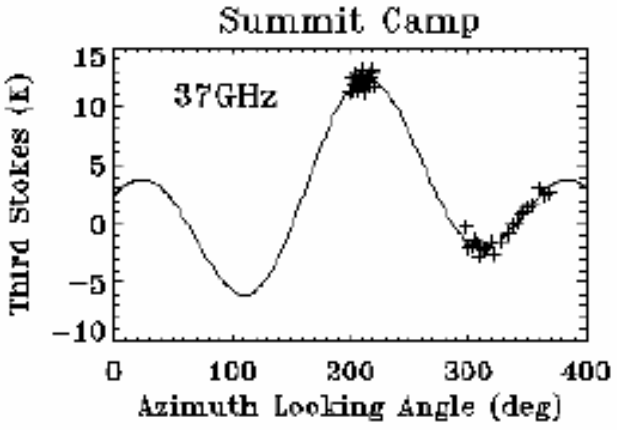

Fourth Stokes parameter

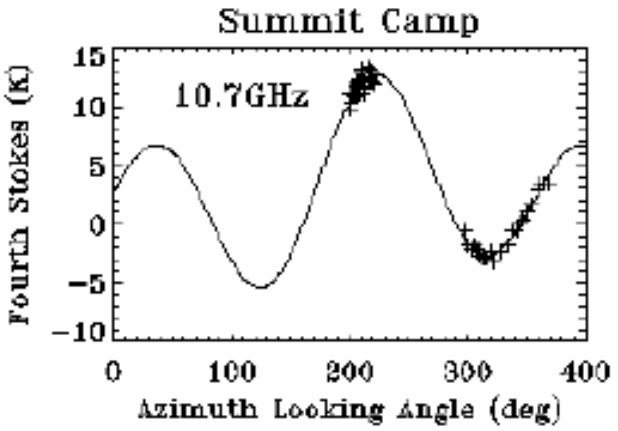

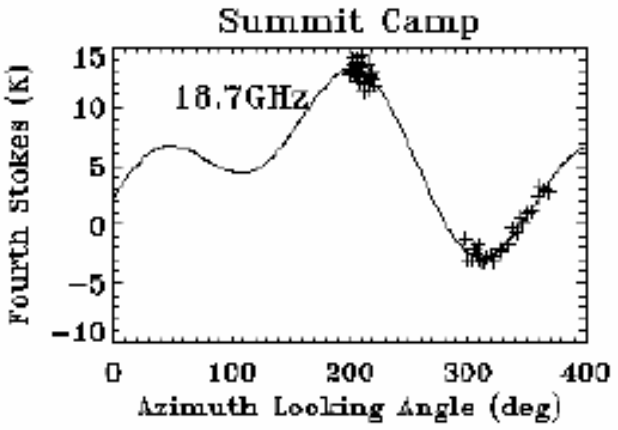

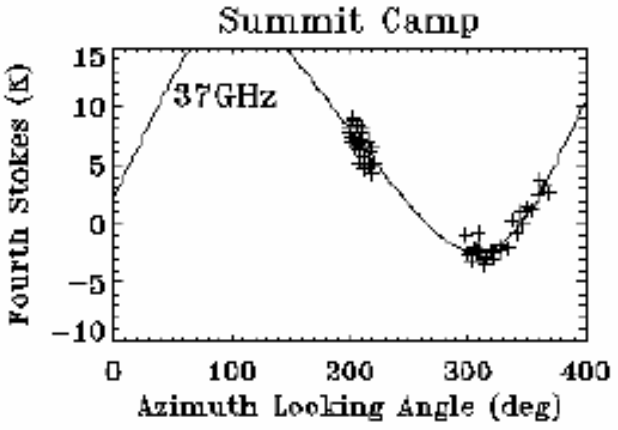

- observed by WindSat over the Summit study site in Greenland during April 2003.
- Large third and fourth Stokes parameters were observed

Sastrugi: Wind induced rough surface

- Aligned rough surface: Aziumthal Asymmetry
- large rms height
- large slope

Third and Fourth Stokes parameters

Past Studies

- Non-spherical particles aligned; Volume Scattering Can Create Large Third and Fourth Stokes parameters
- Smooth surface over layered media: zero 3rd and 4th Stokes parameters
- Azimuthal Asymmetric Rough Surface over half space of snow: Very Small 3rd and 4th Stokes parameters
- Past studies of rough surface scattering have not shown large 4th Stokes parameter

Present Study

- Azimuthal Asymmetric Rough Surface of Snow over Layered media

Numerical Solution of Maxwell equations: Surface Integral equations

$$\hat{y}\cdot\bar{E}_i(\bar{r})+\iint_S dS'\left[\left(\hat{y}\cdot\nabla\times\bar{\bar{G}}\,(\bar{r},\bar{r}')\right)\cdot\left(\hat{n}'\times\bar{E}\,(\bar{r}')\right)+i\omega\mu\;\hat{y}\cdot\bar{\bar{G}}\,(\bar{r},\bar{r}')\cdot\left(\hat{n}'\times\bar{H}\,(\bar{r}')\right)\right]=\begin{cases}\hat{y}\cdot\bar{E}(\bar{r})\\0\end{cases}$$

$$\iint_S dS'\left[\left(\hat{y}\cdot\nabla\times\left(\bar{\bar{G}}_1(\bar{r},\bar{r}')+\bar{\bar{G}}_{1R}^{(m)}(\bar{r}',\bar{r})\right)\right)\cdot\left(\hat{n}'\times\bar{E}_1(\bar{r}')\right)+i\omega\mu\;\hat{y}\cdot\left(\bar{\bar{G}}_1(\bar{r},\bar{r}')+\bar{\bar{G}}_{1R}^{(e)}(\bar{r}',\bar{r})\right)\cdot\left(\hat{n}'\times\bar{H}_1(\bar{r}')\right)\right]=\begin{cases}0\\-\hat{y}\cdot\bar{E}_1(\bar{r})\end{cases}$$

similar equation for magnetic field

- G is dyadic green function in upper half space
- (G_1+G_{1R}) is dyadic function in lower half space
- Periodic boundary condition to account for deep subsurface reflections from layering

Method of Moments convert surface integral equation into matrix equation

$$\begin{bmatrix} \overline{\overline{B}}^{(0)}_{N\times N} & \overline{\overline{A}}^{(0)}_{N\times N} & 0 & 0 \\ \overline{\overline{B}}^{(1)}_{N\times N} & \frac{\tau}{\rho}\overline{\overline{A}}^{(1)}_{N\times N} & (\tau-1)\frac{\upsilon\eta}{\rho}\overline{\overline{C}}^{(1)}_{N\times N} & 0 \\ 0 & 0 & \overline{\overline{B}}^{(0)}_{N\times N} & \overline{\overline{A}}^{(0)}_{N\times N} \\ -(\tau-1)\frac{\upsilon}{\eta}\overline{\overline{C}}^{(1)}_{N\times N} & 0 & \overline{\overline{B}}^{(1)}_{N\times N} & \tau\overline{\overline{A}}^{(1)}_{N\times N} \end{bmatrix} \begin{bmatrix} \overline{\psi}_{N\times 1} \\ \overline{\chi}_{N\times 1} \\ \overline{\varphi}_{N\times 1} \\ \overline{\xi}_{N\times 1} \end{bmatrix} = \begin{bmatrix} \overline{E}^{yi}_{N\times 1} \\ \overline{0}_{N\times 1} \\ \overline{H}^{yi}_{N\times 1} \\ \overline{0}_{N\times 1} \end{bmatrix}$$

(a) non-layer, $\overline{\overline{A}}^{(0)}_{N\times N}$ $\overline{\overline{B}}^{(0)}_{N\times N}$ $\overline{\overline{A}}^{(1)}_{N\times N}$ $\overline{\overline{B}}^{(1)}_{N\times N}$ same as decoupled case

$$\begin{bmatrix} \overline{\overline{B}}_0 & \overline{\overline{A}}_0 & 0 & 0 \\ \overline{\overline{B}}_1 + \overline{\overline{B}}^{(e)}_{1R} & a_1\overline{\overline{A}}_1 + a_{1R}\overline{\overline{A}}^{(m)}_{1R} & c_1\overline{\overline{C}}_1 + c_{1R}\overline{\overline{C}}^{(e)}_{1R} & d_{1R}\overline{\overline{D}}^{(m)}_{1R} \\ 0 & 0 & \overline{\overline{B}}_0 & \overline{\overline{A}}_0 \\ -\rho\left(c_1\overline{\overline{C}}_1 + c_{1R}\overline{\overline{C}}^{(m)}_{1R}\right) & -d_{1R}\overline{\overline{D}}^{(e)}_{1R} & \overline{\overline{B}}_1 + \overline{\overline{B}}^{(m)}_{1R} & \rho\left(a_1\overline{\overline{A}}_1 + a_{1R}\overline{\overline{A}}^{(e)}_{1R}\right) \end{bmatrix} \begin{bmatrix} \overline{\psi}_{N\times 1} \\ \overline{\chi}_{N\times 1} \\ \eta\overline{\varphi}_{N\times 1} \\ \eta\overline{\xi}_{N\times 1} \end{bmatrix} = \begin{bmatrix} \overline{E}^{ywi}_{N\times 1} \\ \overline{0}_{N\times 1} \\ \eta\overline{H}^{ywi}_{N\times 1} \\ \overline{0}_{N\times 1} \end{bmatrix}$$

(b)multi- layered: there reflection terms

Sinusoidal surface : comparison between Kong's MIT group (1992)(no layers) and layered media

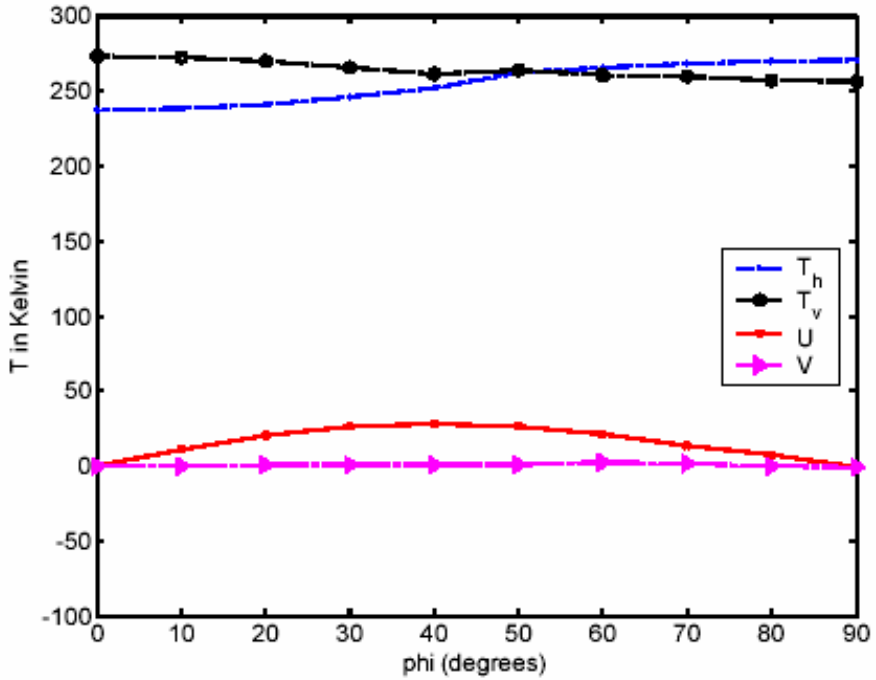

(a) MIT's case

ε_1=12

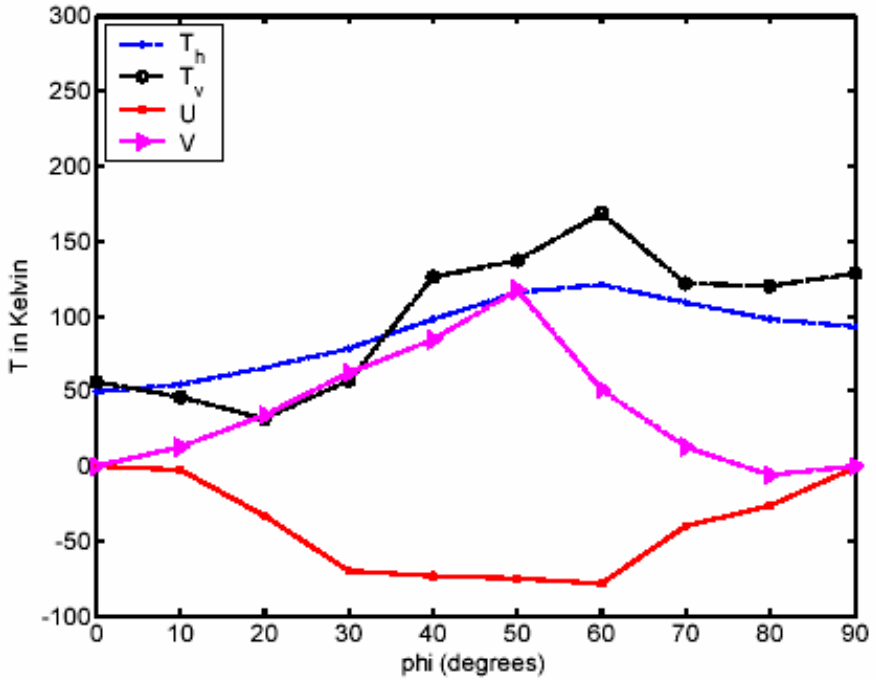

(b) sin-surface over 2 layers media

ε_1=12 , ε_2=1

MIT case (1992): 4th Stokes parameter ~= 0

Present case : 4th Stokes large for rough surface over layered media

Results I for layered snow (effects of total internal reflection)

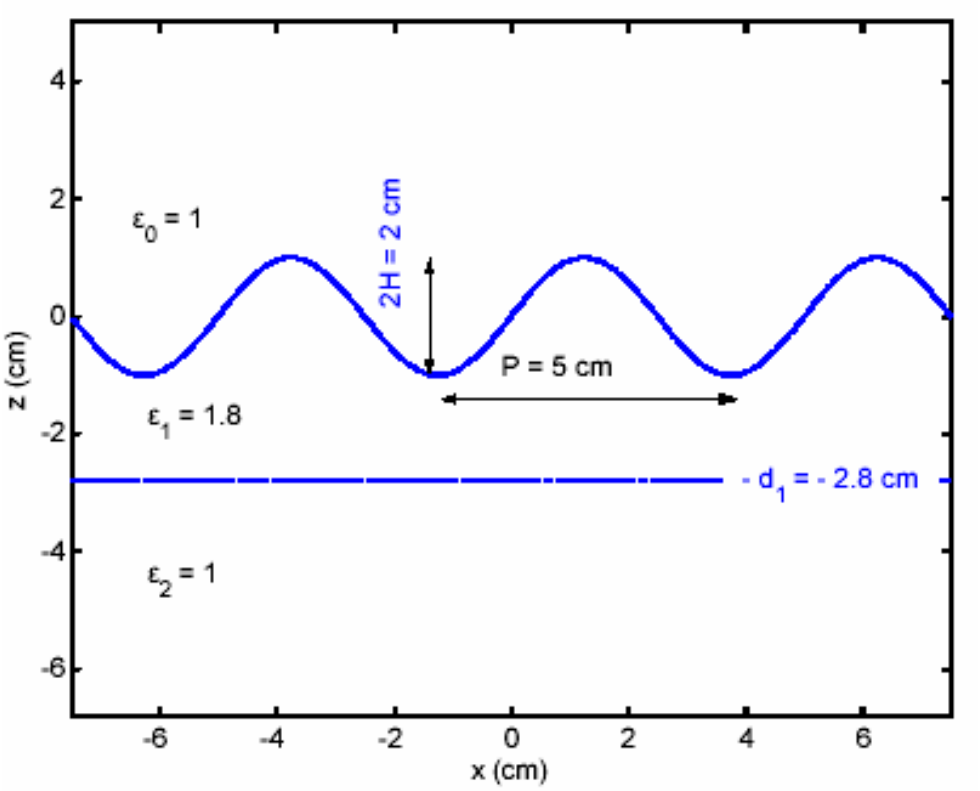

(a) $z = \sin\left(2\pi \frac{x}{5}\right)$ cm, $d_1 = 2.8$ cm

- θ=55 deg.
- Freq = 10 GHz
- 2 layers
- Physical temperature = 250 K
- Total internal reflection

Results I for layered snow (continue)
(four stokes parameters as a function of azimuth angle)

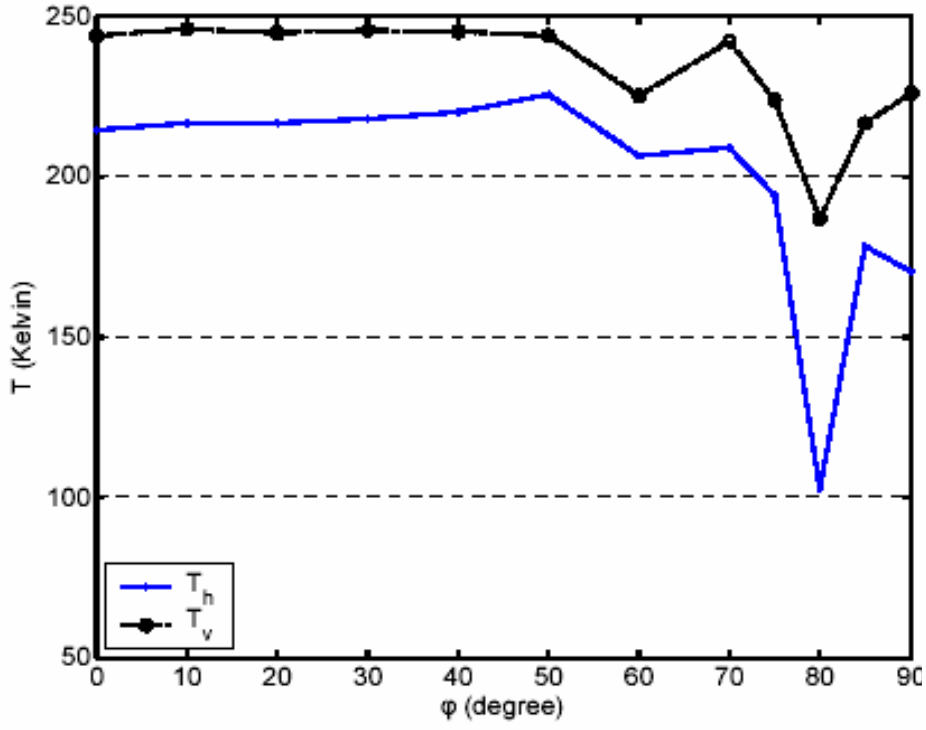

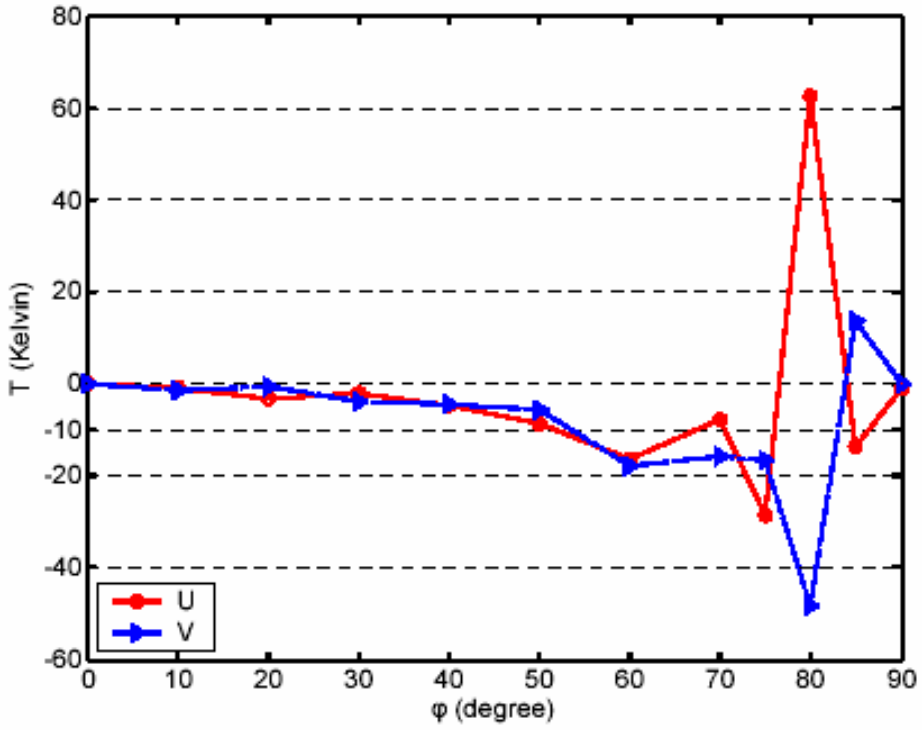

Comparison of results between rough surface and rough surface over 60 layers

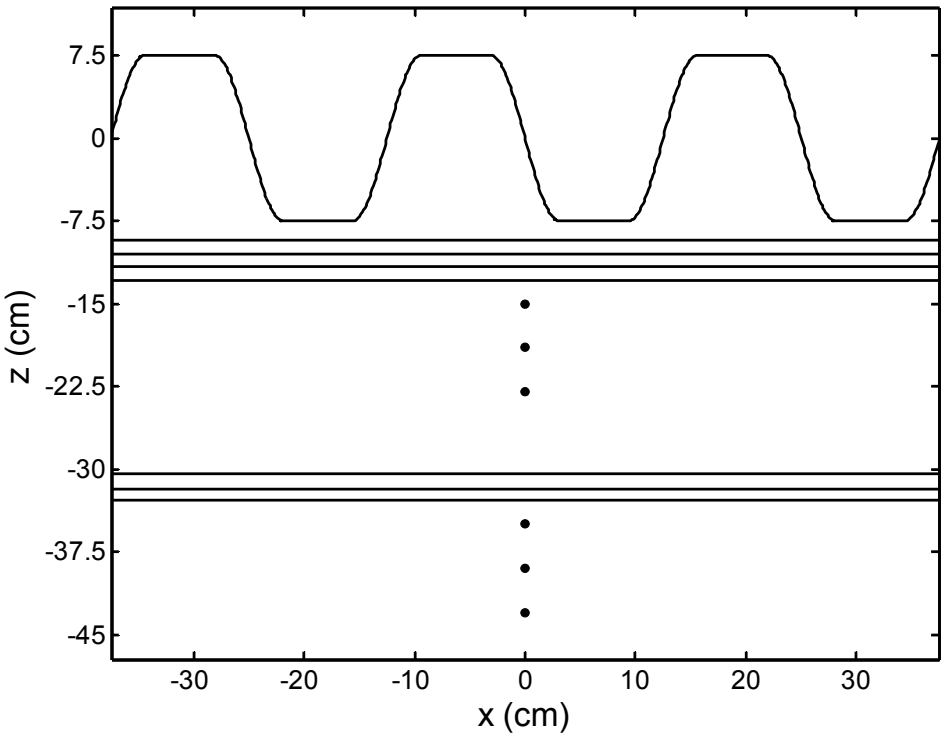

Sastrugi-type rough surface (large slope and large height) over 60 layers (profile)

- Rough surf. Shown in left fig.
- θ=55 deg., Freq = 10 GHz
- Physical temperature = 250 K
- 60 Layers
  - ✓Permmitivity:
    - ➢ε1=1.8+0.0006i
    - ➢ ε2=1.3+0.000325i
    - ➢ε3=1.8+0.0045i
    - ➢ε4=1.6+0.0045i
    - ➢ε5=1.8+0.0045i
    - ➢……
    - ➢ε60=3.2+0.0008i
  - ✓Thickness of each layer:
    - ➢Random between 1~1.5 cm

Comparison of results between rough surface and rough surface over 60 layers (continue)

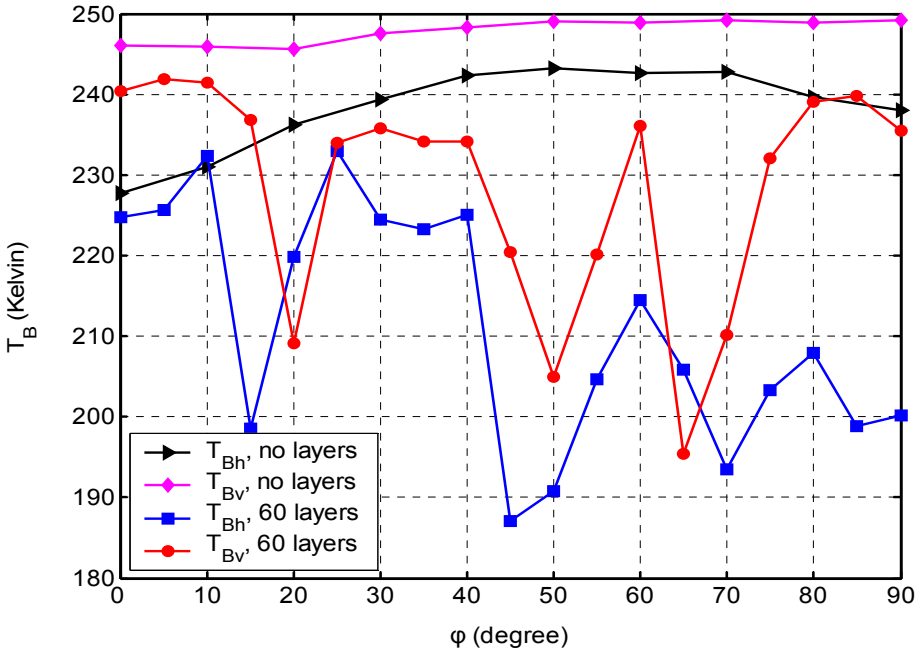

(a) 1st & 2nd Stokes parameters

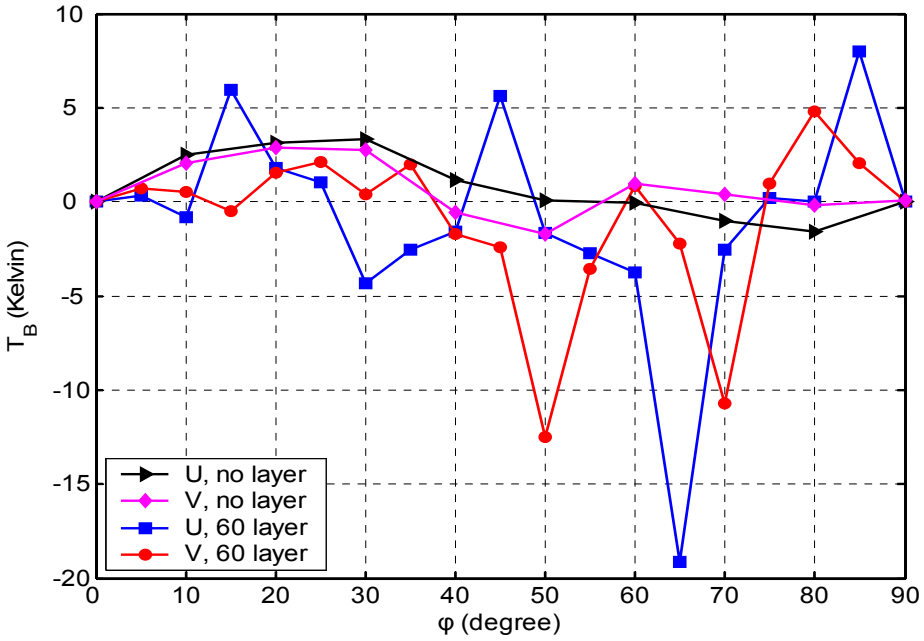

(b) 3rd & 4th Stokes parameters

- one realization
- θ=55 deg., Physical temperature = 250 K
- Freq = 10 GHz
- Th & Tv over layered media smaller than without layers
- U & V over layered media larger than without layers

Summary

1. Volume Scattering with Layering
   1. *QCA/DMRT simulate all 4 channels: 18V, 18H, 37 V and 37 H*
   2. *Comparison with CLPX GBMR ground measurements for all 4 channels to account for frequency depdence and polariation dependence*
2. NMM3D/DMRT
   1. *Numerical Maxwell Model based on 3D Solutions (NMM3D) of Maxwell equations*
   2. *comparison with QCA/DMRT: NMM3D/DMRT has weaker dependence in snow density*
3. Surface Scattering with Layering : Numerical solutions of Maxwell Equations:
   1. *Large 3rd and 4th Stokes may be caused by interactions of rough surface with layering*
   2. *Large 3^{rd} and 4^{th} parameters observed in WINDSAT data over Greenland*